Journal of Nuclear and Radiochemical Sciences, Vol. 6, No.1, pp. 77-80, 2005

Adsorption of Th(IV) and Pu(IV) on the Surface of *Pseudomonas fluorescens* and *Bacillus subtilis* in the Presence of Desferrioxamine Siderophore

Takahiro Yoshida,*,†,[a] Takuo Ozaki,[a] Toshihiko Ohnuki,[a] and Arokiasamy J. Francis[b]

[a]*Advanced Science Research Center, Japan Atomic Energy Research Institute, Tokai, Ibaraki 319-1195, Japan*
[b]*Environmental Sciences Department, Brookhaven National Laboratory, Upto, New York 11973*

Received: November 15, 2004; In Final Form: April 21, 2005

Adsorption of Th(IV) and Pu(IV) on a Gram-negative bacterium *Pseudomonas fluorescens* and a Gram-positive bacterium *Bacillus subtilis* in the presence of siderophore desferrioxamine B (DFO) was studied. Thorium(IV) and Pu(IV) were dissociated from DFO during adsorption on the cells. Thorium(IV) adsorption on bacterial cells in the presence of DFO was larger than that of Pu(IV) because of the smaller stability of the Th(IV)-DFO complex than that of the Pu(IV)-DFO complex. On the other hand, adsorption of Pu(IV) was larger than that of Fe(III), wherein the stability of the Pu(IV)- and Fe(III)-DFO complex is comparable. *P. fluorescens* showed a higher affinity for Th(IV) and Pu(IV) than *B. subtilis*, though potentiometric titration of bacterial cells indicated that surfaces of *P. fluorescens* and *B. subtilis* cells showed similar proton binding properties.

1. Introduction

Migration behavior of actinides in the environment is of great concern in assessing the safety of radionuclide waste disposal. Chelating reagents, derived from biological activity and industrial drainage, have potential to enhance solubility of actinides through complexation.[1, 2] Siderophores are natural chelating reagents, which are produced by microorganisms. They form strong complexes with otherwise insoluble Fe(III) to supply bioavailable Fe as a siderophore complex.[3, 4] Siderophores also form strong complexes with tetravalent actinides and enhance their solubility.[5–7]

Microorganisms adsorb metals complexed with organic ligands[8–10] or degrade metal-organic ligands complexes.[11] The Fe(III)-siderophore complex is not adsorbed on the cell surfaces of microorganisms, such as *Pseudomonas fluorescens*.[10] On the other hand, some microorganisms, such as *Escherichia coli* and *Bacillus subtilis* take up the Fe(III)-siderophore complexes via their transport systems in the cell membrane.[12, 13] John et al. revealed that the Pu(IV)-siderophore complex was recognized by Fe-siderophore uptake systems of *Microbacterium flavescens*.[14] However, interactions of actinides-siderophore complexes with the cell surfaces of microorganisms are not fully known.

In this study, we examined adsorption behavior of Th(IV) and Pu(IV) on microorganisms in the presence of a siderophore to elucidate the influence of microorganisms on the mobility of tetravalent actinides complexed with a siderophore. A Gram-negative bacterium *Pseudomonas fluorescens* and a Gram-positive bacterium *Bacillus subtilis*, both of which are ubiquitous in the environment, were used in this study. We conducted batch experiments for the adsorption of Th(IV) and Pu(IV) on bacteria in the presence of a linear trihydroxamate siderophore, desferrioxamine B (DFO). Bacterial cell surfaces were characterized by means of potentiometric titration in order to estimate the binding property of the cell surfaces of these two bacteria.

*Corresponding author. E-mail: yoshida-takahiro@aist.go.jp. FAX: +81-29-861-3643.

†Present address: Research Center for Deep Geological Environments National Institute of Advanced Industrial Science and Technology Higashi 1-1-1, Tsukuba 305-8567, Japan

2. Experimenl

2.1. Reagents. Desferrioxamine B was purchased from Sigma Co. Ltd. and used without further purification. A Pu(IV) stock solution was prepared by purification using anion exchange resin (Dowex 1-X8) to remove Am. The concentration of Pu(IV) in the stock solution was analyzed by UV-visible spectroscopy. Plutonium was handled in a glovebox. Thorium(IV) nitrate was purchased from Yokosawa Chem. Co. Ltd. and used without further purification.

2.2. Culture. *Pseudomonas fluorescens* (ATCC 55241) and *Bacillus subtilis* (IAM 1069) were grown in rich media containing the following ingredients: beef extract, 3 g L^{-1}; polypeptone, 5 g L^{-1}; and NaCl, 5 g L^{-1}. They were incubated for 2 days at 30 ˚C on a rotary shaker at 100 rpm. The cells were harvested at the stationary phase by centrifugation at 10000 *g* for 5 minutes and washed twice with a 0.1 M NaCl solution.

2.3. Adsorption experiments. The adsorption of Th(IV) and Pu(IV) in the presence of DFO by *P. fluorescens* and *B. subtilis* was measured at pH 3–9 by batch methods. Bacterial cells were contacted with 20 μM of the 1:1 Th(IV)-DFO or Pu(IV)-DFO complexes in 1.5 mL of 0.1 M NaCl solution containing 1 mM tris(hydroxylmethyl)aminomethane (Tris) in centrifuge tubes composed of polypropylene. Biomass used in the experiments was 0.48–0.89 g L^{-1} on a dry weight basis. After adjusting the pH of the suspensions by HCl or NaOH, the suspensions were left to stand at room temperature. Amounts of Th(IV) and Pu(IV) adsorbed on bacterial cells were measured after 3 hours of contact: our preliminary kinetics experiments showed that the adsorption of these elements reached equilibrium within 3 hours. After separating the cells by centrifugation at 5200 *g* for 10 minutes, concentrations of Th and Pu in the supernatant were analyzed. Thorium was analyzed by inductive coupled plasma mass spectroscopy (ICP-MS) (Hewlett Packard, HP4500) and Pu was analyzed by liquid scintillation counting.

Adsorption of DFO bound with Th(IV) on bacterial cells was also examined by the following procedures. *P. fluorescens* cells or *B. subtilis* cells were contacted with 20 μM of the 1:1 Th(IV)-DFO complex. After separating the cells by centrifugation, DFO remaining in the supernatant was analyzed by high pressure liquid chromatography-electrospray ionization-mass spectrometry (HPLC-ESI-MS) as $Fe(III)(HDFO)^{+}$ after allowing

Published on Web 07/31/2005

DFO to complex with Fe(III) by adding 0.5 mL of 100 μM $Fe(III)(NO_3)_3$ solution to 0.5 mL of the supernatant. The concentration of the Fe(III)-DFO complex was determined by HPLC (WATERS, alliance 2695) using an Xterra® C_{18} column (WATERS) with the mobile phase of a mixture of 0.2% (w/v) formic acid and 7.5% (v/v) methanol. For ESI-MS detection, the single-ion recording (SIR) mode was used for $Fe(III)(HDFO)^+$ ion at $m/z = 614.3$ by using mass spectrometer ZQ2000 (WATERS). Adsorption of 20 μM Pu(IV) on *P. fluorescens* cells in the presence of an excess DFO concentration (200 and 2000 μM) was also done.

2.4. Potentiometric titration. The surface of *P. fluorescens* and *B. subtilis* cells was characterized with regard to the site density of the cell surface by means of potentiometric titration. Bacterial cell suspensions containing 3.0 $g_{dry\ weight}\ L^{-1}$ *P. fluorescens* cells or 3.3 $g_{dry\ weight}\ L^{-1}$ *B. subtilis* cells in 50 mL of a 0.1 M NaCl solution were titrated by stepwise addition of 0.01 mL of 0.1 M HCl or carbonate-free 0.1 M NaOH at 3 minutes intervals in an Ar atmosphere at room temperature.

Proton dissociation from the cell surface can be described by the following eq 1

$$HL^0 = H^+ + L^-, \quad (1)$$

where L^- is the amount of proton binding sites on the cell surface. The net surface charge excess expression for a given amount of cells is equal to the difference between the total base added and the equilibrium H^+ and OH^- ion concentration at any given point of the titration curve calculated by eq 2,

$$\text{Charge excess (M } g_{dry\ weight}^{-1}) = (C_a - C_b + [OH^-] - [H^+])/w, \quad (2)$$

where w is the dry weight of the bacterial cells per liter (g L^{-1}); C_a and C_b are concentrations (M L^{-1}) of the added acid and base, respectively; and $[H^+]$ and $[OH^-]$ are the concentrations of H^+ and OH^- (M L^{-1}) calculated from the pH measured. The concentration of proton binding sites (L_T) on the cell surface can be described by the following mass action eq 3

$$K_a = [L^-][H^+]/[HL^0], \quad (3)$$

where K_a is the acidity constant of proton binding sites. The concentrations of proton binding sites and their pK_a values were calculated using the computer program FITEQL 4.0.[15] We adopted a three-site model, which has been widely used for characterization of the bacterial cell surface.[16, 17]

2.5. Speciation of Fe(III) and Th(IV) in DFO system. Speciation of Fe(III) and Th(IV) in DFO ligand was calculated at pH 3–9. Protonation and deprotonation constants of the Fe(III)- and Th(IV)-DFO complexes were used from literatures.[18, 19] Hydrolysis of Fe(III) and Th(IV) is quite strong in aqueous solution. Metal hydroxide species $Th(H_{-1}DFO)$, hydroxylated species of the Th(IV)-DFO complex, was considered in the calculation. However, hydrolysis of Fe(III)-DFO complex was not considered in the calculation because we did not found any thermodynamic data of the hydrolysis of the complex.

3. Results

Figure 1 shows adsorption density of Th(IV) and Pu(IV) on bacterial cells in the presence of DFO. Adsorption of Pu(IV) on *P. fluorescens* cells increased from 3 to 19 μM g^{-1} with a decrease of pH from 7.3 to 3.0 while adsorption of Pu(IV) on *B. subtilis* was smaller than 3 μM g^{-1} at about pH 3–8. Adsorption of Th(IV) on *P. fluorescens* cells and *B. subtilis* cells was larger than that of Pu(IV) on each species. It increased with a decrease in pH.

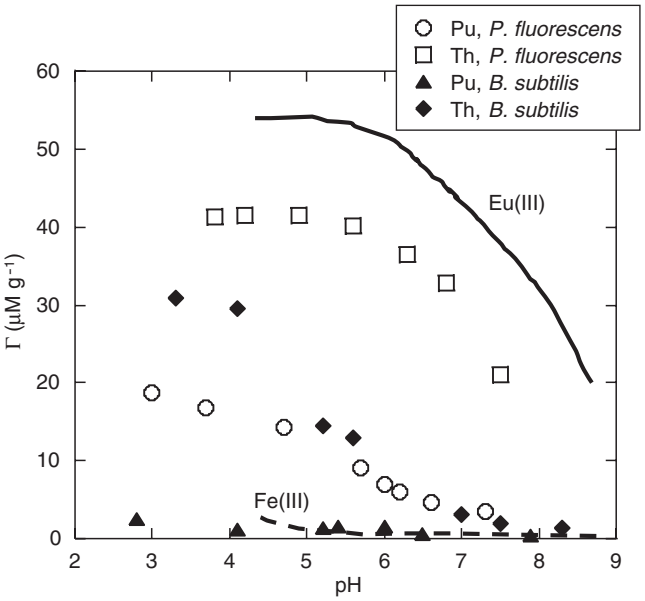

Figure 1. Adsorption density of Th(IV) and Pu(IV) on *P. fluorescens* and *B. subtilis* in the presence of DFO. Initial concentrations of Fe(III), Eu(III), Th(IV), Pu(IV), and DFO were 20 μM. Data for Fe(III) and Eu(III) are plotted based on the reference 10.

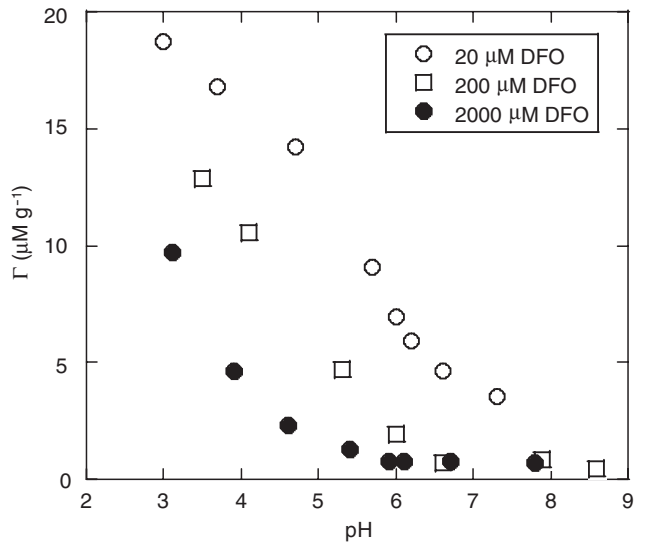

Figure 2. Adsorption density of Pu(IV) on *P. fluorescens* cells at various DFO concentrations.

We also measured percent adsorption of Th(IV) and DFO in 20 μM of the 1:1 Th(IV)-DFO complex solution on 1.7 gL^{-1} *P. fluorescens* cells or 1.6 gL^{-1} *B. subtilis* cells at pH 5.5, showing that *P. fluorescens* adsorbed approximately 97% of Th(IV) and 2% of DFO, while *B. subtilis* adsorbed approximately 91% of Th(IV) and 7% of DFO.

Figure 2 shows adsorption of Pu(IV) on *P. fluorescens* cells at 20, 200, and 2000 μM DFO. Adsorption density of Pu(IV) on *P. fluorescens* cells shows a decreasing tendency with an increase of the DFO concentration from 20 to 2000 μM.

Figure 3 shows charge excess plots of cell surfaces and calculated fitting curves. The point of zero charge (pzc) of *P. fluorescens* and *B. subtilis* surfaces is 7.2 and 7.5, respectively. The calculated concentrations of proton binding sites and pK_a values are listed in Table 1 Calculated weighted sum of squares divided by degrees of freedom (WSOS/DF) values, which can be used as an indicator of the reliability of fitting of potentiometric titration curve drawn by FITEQL, for *P. fluorescens* and *B. subtilis* were 1.0 and 0.7, respectively. Fitting procedures with a WSOS/DF smaller than 20 can be considered to

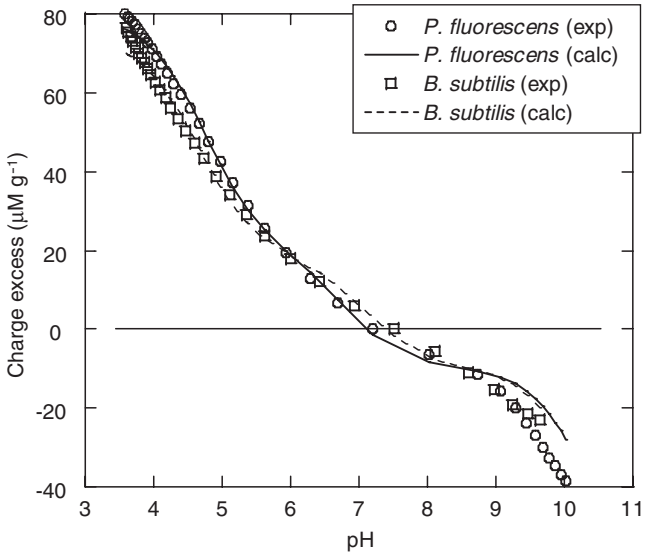

Figure 3. Surface charge excesses of *P. fluorescens* and *B. subtilis* cells. Solid and dotted lines represent best-fitting curves based on the three-site model.

TABLE 1: Summary of Concentrations (L_T) and pK_a Values for the Proton Binding Sites on the Surfaces of *P. fluorescens* and *B. subtilis* Cells

P. fluorescens		functional groups
pK_a	L_T (μmol g^{-1})	
4.8	61	carboxyl
6.8	30	phosphate
10.5	81	amine
B. subtilis		
pK_a	L_T (μmol g^{-1})	
4.6	56	carboxyl
7.1	28	phosphate
10.4	75	amine

be reliable.[15] pK_a values showed that these species had acidic (4.6–4.8), neutral (6.8–7.1), and basic (10.4–10.5) functional groups. Concentrations of these proton binding sites on these two species were almost comparable to each other.

Figure 4 shows calculated speciation of the Fe(III)- and Th(IV)-DFO complex at pH 3–9. The predominant species of the Fe(III)-DFO complex at pH 3–8 is Fe(III)(HDFO)$^+$ and fraction of protonated Fe(III)(H_2DFO)$^{2+}$ is negligible (Figure 4a). The predominant Th(IV)-DFO complex species at pH 3–7 is Th(IV)(HDFO)$^{2+}$ (Figure 4b). Above pH 7.8, more than 50% of the Th(IV)-DFO complex is present as Th(IV)(DFO)$^+$. Five percent of the Th(IV)-DFO complex is present as metal hydroxide species, Th(H_{-1}DFO), at pH 9. At acidic pH, Th(IV)(HDFO)$^{2+}$ is protonated to Th(IV)(H_2DFO)$^{3+}$.

4. Discussion

Thorium(IV) was adsorbed on *P. fluorescens* and *B. subtilis*, while DFO was not adsorbed on them, indicating that the Th(IV)-DFO complex dissociated during the adsorption of Th(IV) on the cells. This finding is in agreement with the result of the Eu(III) adsorption on *P. fluorescens* cells in the presence of DFO: the Eu(III)-DFO complex dissociated and only Eu(III) adsorbed on *P. fluorescens* cells.[10] We did not analyze the DFO concentration in the Pu(IV)-DFO complex solution because of analytical constrains. The decreasing tendency of Pu(IV) adsorption on *P. fluorescens* cells with an increase of DFO concentration (Figure 2) suggests that the surface of *P. fluorescens* cells competes with DFO for Pu(IV). This finding indicates that the affinity of hydrated Pu(IV) with bacterial cells is higher than that of the Pu(IV)-DFO complex, suggesting the dissociation of the Pu(IV)-DFO complex during the Pu(IV) adsorption.

In Figure 1, adsorption of Fe(III) and Eu(III) on *P. fluorescens* cells in the presence of DFO is shown. The lines are illustrated based on published data.[10] Adsorption of Fe(III) on *P. fluorescens* is significantly smaller than that of Th(IV) and Pu(IV). Europium(III) adsorption is higher than those of Th(IV) and Pu(IV). Stability constants of the metal-DFO complexes decrease in the order of Pu(IV) (log K = 30.8)[5] > Fe(III) (log K = 30.6)[18] > Th(IV) (log K = 26.6)[19] > Eu(III) (log K = 15).[6] Adsorption density of Eu(III), Th(IV), and Pu(IV) on *P. fluorescens* cells decreased in the order Eu(III) > Th(IV) > Pu(IV), which corresponds to the increasing order of the stability constant of the DFO complexes. Adsorption of hydrated Eu(III) on *P. fluorescens* cells does not change significantly at pH 3–8,[20, 21] indicating that affinity of *P. fluorescens* cell surfaces with metal ions is not changed significantly at these pHs. These facts indicate that pH dependence of adsorption density of metal ions on cells is dominantly controlled by the stability of the metal-DFO complexes. Chemical speciations of metal-DFO complexes are protonated or deprotonated depending on the solution pH, leading to a different adsorption density of metals on the cells. Three hydroxamate groups in DFO bind Eu(III) above pH 8.1.[10] Below pH 8.1, the Eu(III)-DFO complex successively dissociates with decreasing pH and Eu(III) exists as a hydrated ion at pH < 4, resulting in the

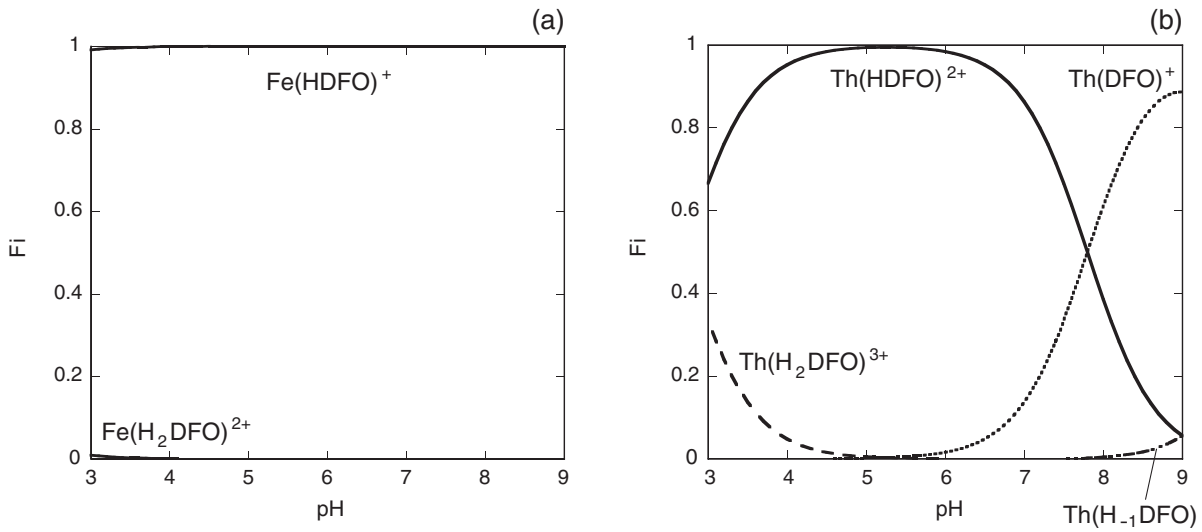

Figure 4. Chemical species of (a) the Fe(III)-DFO and (b) the Th(IV)-DFO complexes as a function of pH.

higher adsorption of Eu(III) on cells at acidic pH.[10]

The Th(IV)-DFO complex is successively protonated or deprotonated with a change of pH. In $Th(IV)(HDFO)^{2+}$, Th(IV) is coordinated with three hydroxamate groups of DFO wherein amine group is protonated. An increase of pH above 7 results in the deprotonation of amine and the change of $Th(HDFO)^{2+}$ to $Th(IV)(DFO)^{+}$. On the other hand, $Th(IV)(HDFO)^{2+}$ is protonated to $Th(IV)(H_2DFO)^{3+}$ with decreasing pH below 4 (Figure 4b), leading to the dissociation of bonds between the hydroxamate group and Th(IV). Stability of the Th(IV)-DFO complex decreases in the order of $Th(IV)(DFO)^{+} > Th(IV)(HDFO)^{2+} > Th(H_2DFO)^{3+}$, resulting in higher adsorption of Th(IV) at lower pH. On the other hand, chemical speciation of the Fe(III)-DFO complex does not significantly change at pH 3–9, resulting in the constantly low adsorption density within the pH range examined.

Adsorption of Pu(IV) on *P. fluorescens* cells was greater than that of Fe(III) (Figure 1), though stability constants of the Fe(III)- and Pu(IV)-DFO complexes are comparable. Ferric iron in a cyclic trihydroxamate siderophore, desferrioxamine E is fully encapsulated, being coordinated with 6 oxygen atoms from 3 hydroxamate groups.[22] On the other hand, Pu(IV) in a desferrioxamine E is coordinated with 9 oxygen atoms from 6 oxygen atoms in 3 hydroxamate groups on one side of Pu(IV) and 3 oxygen atoms from 3 water molecules from the other side[23] because of its larger ionic radius.[24] These facts suggest that structure of DFO complex may affect adsorption of metals on bacterial cells. Functional groups on the cell surface would easily access Pu(IV) in DFO from the side coordinated with water molecules than Fe(III) in DFO. Similarly, Th(IV) with the large ionic radius[24] would be coordinated to DFO from its one side, allowing functional groups of the cell surface easily to access Th(IV) from the other side, resulting in the subsequent Th(IV) adsorption.

pK_a values and concentrations of proton binding sites are almost identical in *P. fluorescens* and *B. subtilis* cells (Table 1). Lipopolysaccharide in the outer cell membrane of Gram-negative bacteria contains carboxyl groups and phosphate groups.[25] Peptidoglycan, a proposed structure of surfaces of Gram-positive bacteria, also contains carboxyl and phosphate groups in their structure.[25] We assigned acidic and neutral functional groups of bacterial cell surfaces to carboxyl and phosphate groups, respectively (Table 1). The basic group on bacterial cell surfaces is assigned to amine functional group, found as a component on bacterial cell surfaces.[25] Although the structure and chemical composition of the bacterial cell surfaces are not identical in the Gram-negative and the Gram-positive bacteria, *P. fluorescens* cells and *B. subtilis* cells show similar proton binding properties to each other. It is also reported that a wide range of bacterial species, such as Gram-negative bacteria, *E. coli* and *P. aeruginosa*, and Gram-positive bacteria, *B. subtilis* and *Streptococcus faecalis*, show comparable pK_a of surface functional groups and their concentrations.[26] However, *P. fluorescens* cells had a higher affinity with Th(IV) and Pu(IV) than *B. subtilis* cells (Figure 1), indicating that the affinity of bacterial cell surfaces with tetravalent actinides is not completely correlated with their affinities with proton.

P. fluorescens and *B. subtilis* adsorbed Th(IV) and Pu(IV) in the presence of DFO from solution. Thorium(IV) and Pu(IV) are adsorbed on bacterial cells as a dissociated ion. DFO forms strong complexes with tetravalent actinides, whose stability constants are comparable to that of the Fe(III)-DFO complex. However, adsorption behavior of tetravalent actinides on cells in the presence of DFO is controlled by not only the stability constant of the DFO complexes but also chemical speciation and structure of cell surfaces. Microorganisms in the environment have the potential to affect the movement of tetravalent actinides-DFO complexes by adsorption on their cells.

References

(1) J. F. McCarthy, K. R. Czerwinski, W. E. Sanford, P. M. Jardine, and J. D. Marsh, J. Contam. Hydrol. **30**, 49 (1998).
(2) N. L. Hakem, E. R. Sylwester, and P. G. Allen, J. Radioanal. Nucl. Chem. **250**, 47 (2001).
(3) J. B. Neilands, Annu. Rev. Biochem. **50**, 715 (1981).
(4) A. Albrecht-Gary and A. L. Crumbliss, *Iron Transport and Storage in Microorganisms, Plants, and Animals*, eds. A. Sigel and H. Sigel, Marcel Dekker, New York (1998), p. 239.
(5) N. V. Jarvis and R. D. Hancock, Inorg. Chim. Acta **182**, 229 (1991).
(6) J. R. Brainard, B. A. Strietelmeier, P. H. Smith, P. J. Langston-Unkefer, M. E. Barr, and R. R. Ryan, Radiochim. Acta **58/59**, 357 (1992).
(7) C. E. Ruggiero, J. H. Matonic, S. D. Reilly, and M. P. Neu, Inorg. Chem. **41**, 3593 (2002).
(8) S. Markai, G. Montavon, Y. Andres, and B. Grambow, Appl. Radiat. Isot. **58**, 161 (2003).
(9) T. Yoshida, T. Ozaki, T. Ohnuki, and A. J. Francis, Chem. Geol. **212**, 239 (2004).
(10) T. Yoshida, T. Ozaki, T. Ohnuki, and A. J. Francis, Radiochim. Acta **92**, 749 (2004).
(11) A. J. Francis, C. J. Dodge, and J. B. Gillow, Nature **356**, 140 (1992).
(12) R. Schneider and K. Hantke, Mol. Microbiol. **8**, 111 (1993).
(13) V. Braun and M. Braun, Curr. Opin. Microbiol. **5**, 194 (2002).
(14) S. G. John, C. E. Ruggiero, L. E. Hersman, C. S. Tung, and M. P. Neu, Environ. Sci. Technol. **35**, 2942 (2001).
(15) A. L. Herbelin and J. C. Westall, *FITEQL 4.0: a Computer Program for Determination of Chemical Equilibrium Constants from Experimental Data*, Oregon State University, Corvallis (1996).
(16) A. C. C. Plette, W. H. Riemsdijk, M. Benedetti, and A. Wal, J. Colloid Interf. Sci. **173**, 354 (1995).
(17) N. Yee, L. G. Benning, V. R. Phoenix, and F. G. Ferris, Environ. Sci. Technol. **38**, 775 (2004).
(18) G. Schwarzenbach and K. Schwarzenbach, Helv. Chim. Acta **46**, 1390 (1963).
(19) D. W. Whisenhunt, M. P. Neu, Z. Hou, J. Xu, D. C. Hoffman, and K. N. Raymond, Inorg. Chem. **35**, 4128 (1996).
(20) T. Yoshida, T. Ozaki, T. Ohnuki, and A. J. Francis, *Proc. intern. Symp. on Radioecology and Environmental Dosimetry*, eds. J. Inaba, H. Tsukada, and A. Takeda, Institute of Environmental Sciences, Aomori, Japan (2003), p. 296.
(21) Y. Suzuki, T. Nankawa, T. Yoshida, T. Ozaki, T. Ohnuki, A. J. Francis, S. Tsushima, Y. Enokida, and I. Yamamoto, J. Nucl. Radiochem. Sci. in press.
(22) D. van der Helm and M. Poling, J. Am. Chem. Soc. **98**, 82 (1976).
(23) M. P. Neu, J. H. Matonic, C. E. Ruggiero, and B. L. Scott, Angew. Chem. Int. Ed. **39**, 1442 (2000).
(24) R. D. Shannon and C. T. Prewitt, Acta Cryst. **B25**, 925 (1969).
(25) I. C. Hancock, *Microbial Cell Surface Analysis*, eds. N. Mozes, P. S. Handley, H. J. Busscher, and P. G. Rouxhet Wiley, New York (1991), p. 21.
(26) N. Yee and J. Fein, Geochim. Cosmochim. Acta **65**, 2037 (2001).